2024 IEEE International Conference on Robotics and Automation (ICRA 2024)
May 13-17, 2024. Yokohama, Japan

Design and Characterization of a Soft Flat Tube Twisting Actuator

Hao Liu, Changchun Wu, Senyuan Lin, and Yonghua Chen*, *Member, IEEE*

***Abstract*—Soft actuators have shown advantages of adaptiveness, large deformation, and safe human-robot interaction, making them suitable for various applications. Herein, a novel soft flat tube twisting actuator (SFTTA) is proposed. The SFTTA is composed of a folded flat tube sandwiched between two silicone rubber laminates. When inflated by compressed air, the folded corners of the flat tube tend to unfold, resulting in the twist of the actuator to a helical structure. The SFTTA has great scalability. It can be fabricated through simple processes with low-cost materials. For a sample SFTTA with the size of a human finger, it can twist 540^0 at an air pressure of 300 kPa. In general, SFTTA based actuators can twist 9.6 degree per millimeter in length, which is significantly larger than previously reported soft twisting actuators. Additionally, the composite-like SFTTA allows mechanical property programming through the alteration of folding patterns of the flat tube and the material structure of the elastomer laminates. Finally, an extensible soft gripper based on flat tube actuators and a robotic wrist module are developed, and their rotation is realized by the proposed SFTTA actuator.**

I. Introduction

Soft robots based on various actuation principles are widely used in dexterous manipulation [1-3], safe rehabilitation devices [4,5], vivid biomimetic robots [6,7], and locomotion robots adapted to complex environments [8,9], due to the characteristics of large deformation and high adaptability. Different from the conventional rigid robots with complex and bulky linkage mechanisms with multiple joints, soft robots can effortlessly achieve flexible and compliant motions. Although bending, contracting, and extending actuations of soft robots have been widely studied in recent years, there is limited research on soft twisting or torsional actuators [10-13].

The twisting motion plays a vital role in providing a rotational degree of freedom (DOF) in natural creatures and robotic design. In the human body, we rotate our elbow joints to facilitate the twisting of the forearm and to adjust the attitude of our hands, thereby enabling flexible interaction with the surrounding environment. For robotic end-effectors, the robotic wrist is required to adjust the end-effector to align with targets [14,15].

In recent years, researchers have reported several soft pneumatic twisting actuators. Three types of pneumatic twisting actuators, by arranging flexible chambers to a helix structure, were proposed by Sanan et al, but the maximum rotatory angle of these actuators is only 40 degrees [16]. Researchers also found that the soft actuator constituted of spiral chambers can twist not only in positive pressure but also be driven by vacuum [17-19]. Chen *et al.* optimized the soft twisting pneumatic actuators with a bi-directional twisting rotation of 116.7º (85.3º at positive pressure and 31.4° at negative pressure) [18]. In addition, Kurumaya *et al.* presented a cylindrical soft robotic wrist based on the concept of fiber-reinforced soft actuator and applied it in deep sea manipulation, which could generate a 90-degree rotation [15]. Based on the polydimethylsiloxane (PDMS) soft lithography techniques, Gorissen et al. fabricated a flexible pneumatic twisting actuator with a small size and extremely high twisting angle per actuator length (6.5 º/mm) [20]. However, this actuator cannot bear high pressure (maximum 180 kPa) constrained by the strength of the bond of PDMS layers, and the overall twisting angle is only 110º .

Smart materials have also been widely used in the design of soft actuators. Waters *et al.* used photoresponsive liquid crystalline elastomers (LCEs) to design an actuator triggered by ultraviolet (UV) light, which exhibits simultaneous bi-directional twisting [21]. The LCE actuator can twist 65.5 degrees in both clockwise and anticlockwise directions, and the twisting angle and twisting direction of the actuator can be controlled by the incident azimuthal angle of the light. Shim *et al.* invented a twisting actuator by inserting a prestrained shape memory alloy (SMA) wire into a PDMS matrix [22]. The actuator based on the SMA can rotate 270º , but the high electric current (12.5 A) and slow response (10s) are always the disadvantages of the SMA actuation.

Very few actuators, except some soft actuators with origami structures, can twist themselves more than one turn (i.e., 360º) [13]. Although assembling twisting actuators in series can increase the twisting angle, this also increases the size and decreases response speed. In general, researchers typically evaluate the rotational capability of an actuator in terms of twisting angle per millimeter.

The main contribution of this study is the design of a novel composite-like soft flat tube twisting actuator (SFTTA) as shown in Fig. 1. Nine SFTTA samples with different flat tube folding helix angles, aspect ratio (length/width), elastomer hardness, and wall thickness are fabricated to experimentally study the characteristics of the proposed soft twisting actuator. Results have shown that SFTTAs have great twisting capability (540 degrees in 300 kPa). Besides, the SFTTAs also

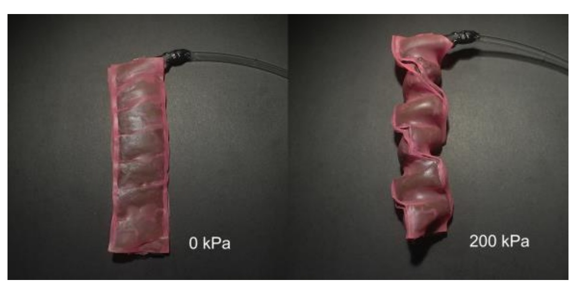

Figure 1. A sample of soft flat tube twisting actuator.

This work is supported by Research Grants Council of the Hong Kong Special Administrative Region, China (Project no. [T42-717/20-R]).

All authors are with the Department of Mechanical Engineering, the University of Hong Kong, Hong Kong, China
*Corresponding author. e-mail: yhchen@hku.hk.

979-8-3503-8457-4/24/$31.00 ©2024 IEEE

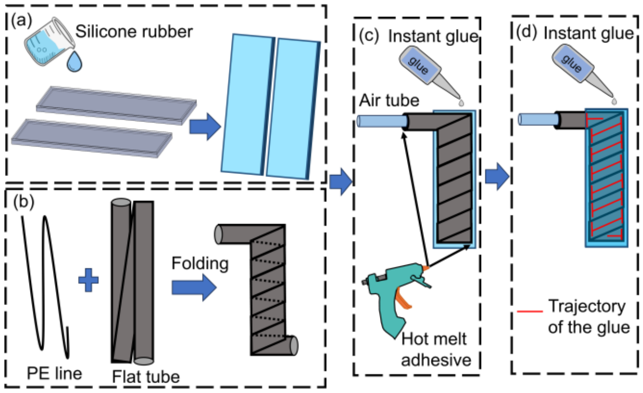

Figure 2. Fabrication of the SFTTA. (a) Mold the silicone rubber laminate. (b) Insert PE line into the flat tube and fold the flat tube with a helix angle. (c-d) Seal the flat tube and glue the flat tube to elastomer laminates.

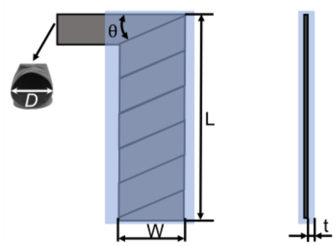

Figure 3. Major parameters of the SFTTA.

have great scalability spanning one order of magnitude to meet requirements in different scenarios. The largest twisting capability of 9.6 °/mm is recorded in the experiments. By changing the folded pattern and material of elastomer laminate, the SFTTA can be used as soft extending and bending actuators. Finally, a robotic gripper consisting of three types of actuators is designed to demonstrate the multiple DOF grasping manipulation, and a robotic wrist based on the SFTTA is presented.

The following part of the paper is organized as follows: Section II presents the design and fabrication of the SFTTA. Section III demonstrates the experimental characterization of the SFTTA including the twisting angle, torque, and response time tests. Section IV highlights the advantages of the SFTTA and shows the extending and bending actuators derived from the SFTTA, a soft gripper and a robotic wrist module are designed to show the potential application of the SFTTA. Section V concludes this paper and provides a discussion about future works.

II. Design and Fabrication of the SFTTA

A. *Design of the SFTTA*

The flat tube used in our study is an off-the-shelf ethylene vinyl acetate (EVA) heat shrink tube. When sealing the ends of the flat tube and inflating it, the width of the flat tube will contract, and the flat side of the tube will bulge, which phenomenon is also widely used to design Peano actuators to generate a contractile motion [16,23].

Here, we propose a novel soft flat tube twisting actuator (SFTTA) constructed by a folded flat tube sealed in a silicone rubber laminate (Fig. 1). At the initial state, the SFTTA is a flexible sheet. When inflating the SFTTA, the flat tube bulges

TABLE I. Parameters of Sample SFTTA actuators

Actuator no.	Parameters			
	Helix angle θ	***Aspect ratio L/W***	***Elastomer Hardness***	***Elastomer layer thickness t***
1(Baseline)	20°	3.5	0 D	1 mm
2	30°	3.5	0 D	1 mm
3	40°	3.5	0 D	1 mm
4	20°	2.3	0 D	1 mm
5	20°	1.75	0 D	1 mm
6	20°	3.5	10 D	1 mm
7	20°	3.5	20 D	1 mm
8	20°	3.5	0 D	0.5 mm
9	20°	3.5	0 D	1.5 mm

and each folded corner tends to unfold to generate a partial rotation [24]. With the synergy of rotation of all folds, the global SFTTA twists and looks like a single-stranded ribonucleic acid (RNA) helix structure. After deflating, the SFTTA will return to its initial state due to the elastic force of the elastomer.

B. *Manufacturing process of the SFTTA*

The structure of the SFTTA is like the sandwich-structured composite materials, as it comprises a folded flat tube core and two elastomer laminates. Fig. 2 shows the manufacturing process of the SFTTA, which can be divided into four steps as follows.

Step I: Pouring the uncured silicone rubber into the 3D-printed rectangular mold and waiting 4 hours to get the silicone rubber laminate. Using an oven to heat the mold could reduce the cure time to 40 minutes.

Step II: To keep the smooth airflow during inflation and deflation, a polyethylene (PE) fishing line is inserted into the flat tube. Folding the flat tube to a helix structure and flattening it.

Step III: Gluing the folded flat tube on a silicone rubber laminate and sealing the ends of the flat tube using the sealed using EVA hot melt adhesive. Due to the similar material of the flat tube and adhesive, the SFTTA shows great airtightness.

Step IV: Finally, gluing another silicone rubber laminate on the SFTTA, and the trajectory of the glue (XH-2029 EVA glue, Dongguan Xinhui Adhesive, CN) is shown in Fig. 2(d). The Supplementary Movie shows more details about the fabrication of the SFTTA.

III. Experimental Characterization of the SFTTA

A. *Parameters of the SFTTA.*

By changing the geometrical parameters of the SFTTA (Fig. 3) and the material of the elastomer, the performance of the SFTTA can be optimized and selected to satisfy various application scenarios. In this study, 9 SFTTA samples are fabricated to explore the effects of helix angle θ, aspect ratio L/W, hardness of elastomer, and wall thickness of the elastomer layer t. The parameters of the 9 samples are shown in Table 1. The actuator sample no.1 is defined as the baseline actuator, and other actuator prototypes only changed one parameter to explore the effect of this parameter on twisting angle and torque output. All 9 SFTTA samples used in the test are in length of 105 mm. All EVA heat shrink tubes used in SFTTA fabrication for experiments in this section are the same with a diameter D of 8 mm and a wall thickness of 0.15 mm. The twisting direction of the SFTTA is determined by the direction of the flat tube helix. All SFTTAs in this section are right-handed, and the SFTTA rotates counterclockwise by inflating when we look from above (i.e., from the side of the air tube).

B. *Twisting angle test of the SFTTA*

To experimentally characterize the effect of the SFTTA on the non-load twisting motion under different pressure inputs, an experiment platform was built as Fig. 4(a), which mainly consists of an air tank, a pressure regulator, a fixture, a clamp, and a camera. One end of the tested SFTTA was fixed on the fixture using a clamp, and another end was twisted free during the test. For the twisting angle test, the air pressure increased from 0 to 200 kPa. For every 20 kPa increment, the SFTTA bottom was captured by a camera, and the picture of the SFTTA bottom was analyzed using the software Image J as Fig. 4(b). The twisting angle test for each sample was conducted three times, and the average twisting angles together with error bars are plotted in Figs. 4(c-f).

Fig. 4(c) presents the twisting angle of the SFTTA (samples no.1, 2, and 3) with different helix angles. The result indicates that a decrease in the helix angle of the SFTTA leads to an increase in the actuated twisting angle, which can be attributed to a larger helix angle resulting in a reduction in the number of loops and folded corners in the same actuator length. For actuators no. 2 and 3, the larger helix angles also reduce the mutual contact of the flat tube on each folded corner. The reduction in the contact area of the flat tube on each folded corner resulting from the decrease in helix angle leads to a decrease in the actuation torque of the pressure acting on the folded corner, which ultimately results in a smaller twisting angle.

Three SFTTAs with widths of 30 mm, 45 mm, and 60 mm (corresponding to samples no.1, 4, and 5, respectively) were manufactured to evaluate the effect of the aspect ratio on the SFTTA performance. As shown in Fig. 4(d), the larger the aspect ratio, the larger the twisting angle. Although the smaller aspect ratio increases the contact area of the flat tube on each folded corner, the corresponding area increment of the elastomer laminate is larger than the contact area increment. Consequently, a larger pressure input and actuation torque are necessary on each folded corner to deform the silicone rubber.

The hardness and the wall thickness *t* of the silicone rubber laminate affect the stiffness of the SFTTA. Figs. 4(e, f) show that when the hardness of the silicone rubber or the thickness of the silicone rubber layer is increased, the twisting angle of the SFTTA at the same air pressure will decrease. The results can be explained by the principle of virtual work [25]:

$$\partial W_p + \partial W_e = 0, \quad (1)$$

in which ∂W_p denotes the work done by air pressure in the flat tube, ∂W_e represents the change of the elastic potential energy of the silicone rubber laminate. In the process of twisting the SFTTA, the silicone rubber laminate undergoes simultaneous stretching and twisting. The deformation of the elastomer layer requires more energy when the elastomer layer is made of harder material or has a thicker wall.

C. *Torque test of the SFTTA*

An experiment test rig was built for testing the torque output of the SFTTA (Fig. 5(a)). One end of the tested SFTTA was fixed on the fixture using a clamp, another end was connected to a torque sensor (0.2 Nm S002 torque sensor, Tianjin STBD Technology, CN). The pressure of the SFTTA was controlled by a pressure regulator, and the torque output value was read on the digital display. Same as the twisting angle test, 9 samples (Table 1) were tested to evaluate the

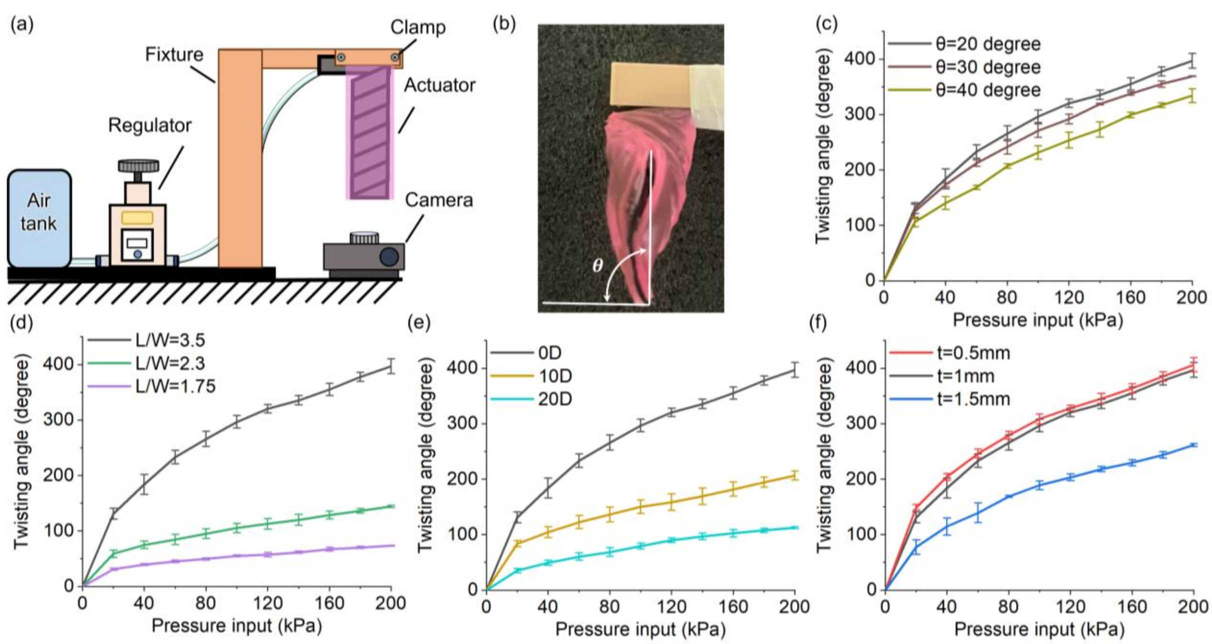

Figure 4. Twisting angle test of the SFTTA. (a) Twisting angle test platform. (b) Measurement of the twisting angle. (c) Effect of the helix angle. (d) Effect of the aspect ratio. (e) Effect of the hardness of the elastomer laminate. (f) Effect of the wall thickness of the elastomer laminate.

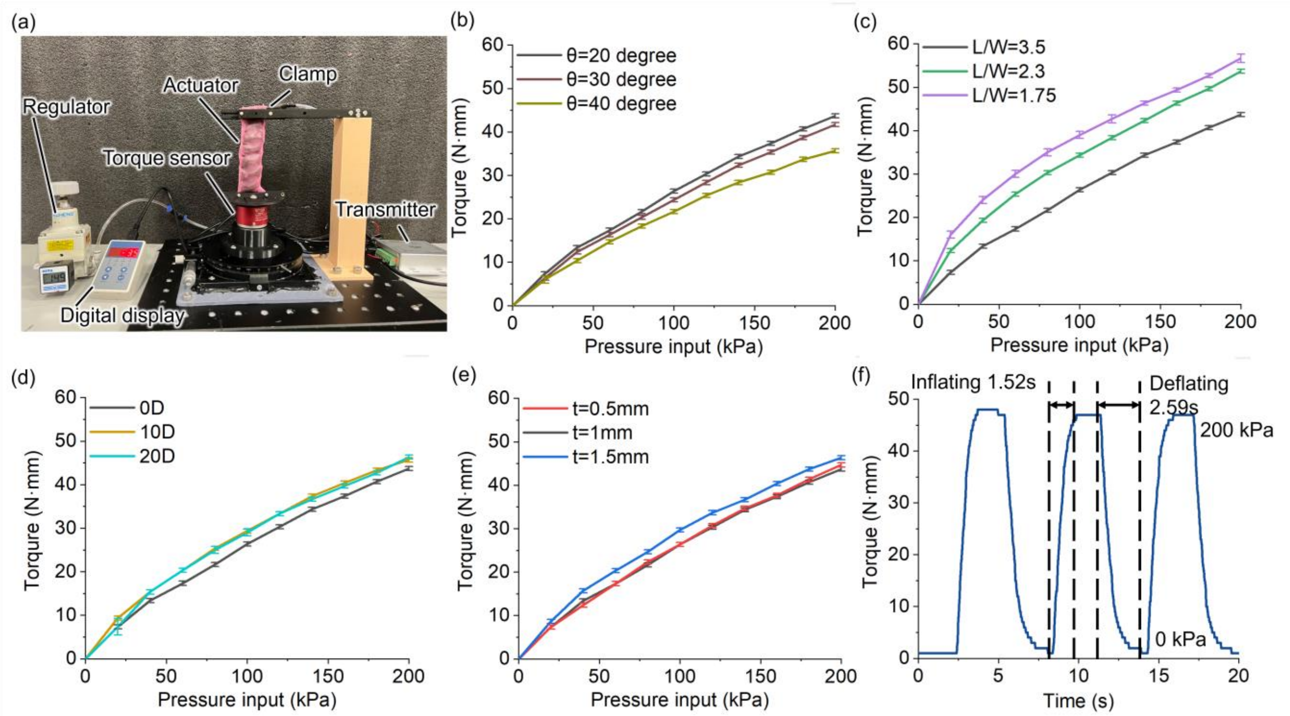

Figure 5. Torque test and dynamic response test of the SFTTA. (a) Experiment test rig for torque test. (b) Effect of the helix angle. (c) Effect of the aspect ratio. (d) Effect of the hardness of the elastomer laminate. (e) Effect of the wall thickness of the elastomer laminate. (f) Dynamic response of the SFTTA.

effect of helix angle θ, aspect ratio L/W, hardness of elastomer, and wall thickness of the elastomer layer t on the torque output. During the torque test, SFTTAs were pressurized from 0 to 200 kPa. For each 20 kPa increment, the torque output of the SFTTA was recorded. The torque test was performed thrice, and the mean twisting angles, along with their corresponding error bars, are depicted in Figs. 5(b-e).

The torque output of the SFTTA is dependent on both the pressure input and the contact area of folded corner. For the SFTTAs with different helix angles (samples no.1, 4, and 5), decreasing the helix angle will increase the contact area of the flat tube on each folded corner, and the SFTTA output larger torque as show in Fig. 5(b). Similarly, increasing the width of the SFTTA, i.e., reducing the aspect ratio, also leads to an increase in the pressure area and a larger torque output (Fig. 5(c)). When both ends of the SFTTA were fixed, there was no obvious rotation on each folded corner. So, the stiffness of the elastomer laminate hardly affected the torque output when the SFTTA was fixed without any twist as shown in Figs. 5(d, e).

For some cases that require a high twisting angle, the SFTTA with a small helix angle, high aspect ratio, and flexible elastomer layer can be selected. Notably, too thin layer thickness of the elastomer wall or too flexible elastomer will cause ultra-soft structure and terrible hysteresis. In some applications, force output is prior. Using a higher aspect ratio and smaller helix angle can significantly improve the force output.

D. *Dynamic response test*

A dynamic response time test was designed to evaluate the response time of the baseline SFTTA during inflating. The testing platform is similar to the torque test platform with small changes. Throughout the experiment, a pressure input of 200 kPa was applied using a pressure source, while the exchange frequency of the inflating and deflating cycles was regulated by a solenoid valve. The data on the torque was acquired by a commercial data acquisition (DAQ) software with a sampling rate of 44Hz.

The result of the dynamic response test is shown in Fig. 5 (f). Actuating the SFTTA from the initial state to the maximum torque requires 1.52 seconds, and the recovery time is almost 2.59 seconds. The response time of the SFTTA strongly depends on the air supply and the parameters of the flat tube. The larger the volume of the actuated flat tube, the longer the time required to fully actuate the SFTTA.

IV. Advantages and Potential Development of the SFTTA

A. *Scalability of the SFTTA*

The SFTTA has an extremely simple structure and manufacturing process, and the primary material, flat tube, is low-cost and readily available. The size of commercially available flat tubes varies from a few millimeters to several hundred millimeters. Besides, based on 3D printing technology, silicone rubber laminate molds with lengths and widths ranging from a few millimeters to hundreds of millimeters can be easily made. Fig. 6(a) demonstrates four SFTTAs with sizes spanning one order of magnitude. The largest actuator is as long as a human forearm, whereas the smallest SFTTA is comparable to the dimensions of a phalanx in a human finger.

The minimum-sized flat tube, constructed from an EVA heat shrink tube featuring a 2 mm diameter (with a wall thickness of 0.2 mm), can bear a pressure of 400 kPa, while also twisting 230 degrees under this pressure as Fig. 6(b).

Under a pressure of 300 kPa, the baseline SFTTA can twist up to 540 degrees. The largest SFTTA comprises an EVA heat shrink tube with a 16 mm diameter and 0.35 mm wall thickness, which can twist 230 degrees under 200 kPa pressure. The increase in size of SFTTA reduces its ability to withstand high pressure.

B. Extending and bending actuators derived from the SFTTA

For sandwich-structured composite materials, changing the core structure and the material of the lamina can optimize material properties. Inspired by composite materials, changing the SFTTA folded corner direction from the 2D helix structure to the 2D zigzag structure can get a soft flat tube extending actuator (SFTEA) as shown in Fig. 7(a). Within the zigzag structure, the rotations occurring at the folded corners are counterbalanced by the opposite rotation of adjacent folded corners during inflation. Consequently, the SFTEA demonstrates extending deformation.

By mixing an inextensible layer with one silicone rubber laminate, the soft extending motion will be transferred to bending motion, and the actuator is named the soft flat tube bending actuator (SFTBA) (Fig. 7(b)). The motions of the SFTEA and SFTBA are shown in the Supplementary Movie.

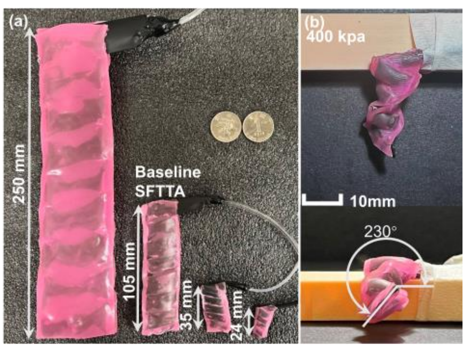

Figure 6. SFTTAs with scalable sizes. (a) SFTTAs of sizes spanning one order of magnitude. (b) Twisting angle of the smallest SFTTA under 400 kPa.

C. Robotic gripper based on the soft flat tube actuators

A soft gripper is designed to demonstrate the application of the SFFTA in robotic manipulations as shown in Fig. 7(c). The extension and contraction of the gripper are achieved by the SFTEA through inflating and deflating it. The fingers of the gripper are made of two SFTBAs. For the two-finger gripper, a rotational DOF is required to align the gripper with objects, especially for objects with sheet-like shapes. The section of SFTTA can adjust the direction of the gripper to align with the target. Figs. 7(d-i) demonstrate that the gripper is aligned to better grasp the objects and rotates the object after grasping.

D. Robotic wrist based on the SFTTA

We designed a robotic wrist module based on the SFTTA in Fig. 8(a). The unique hollow structure of the SFTTA allows inserting a rigid rod into the SFTTA to overcome the ultra-soft construction and make the SFTTA more practical in diverse scenarios. In addition, the twisting motion of the SFTTA does not exists parasitic motion in the longitudinal direction, which means that both ends of the actuator can be fixed in a certain distance. Two elastic bands are connected on the double sides of the module to provide a fast and precise return motion as show in the Supplementary Movie. A hand model (200g) is assembled on the robotic wrist module, and it can be rotated almost 100 degrees at 300 kPa pressure input, like Figs. 8(b-d).

V. Discussion and Conclusion

This research proposed a composite-like novel soft twisting actuator, namely the soft flat tube twisting actuator (SFTTA). Different from previous research, whose torsion morphing mostly relies on the elastic deformation of the material restricted by constraining layers or preprogrammed structures, the torsion of SFTTA is realized by unfolding the pre-folded flat tube, which enables a larger torsion angles output. The SFTTA presents a great scalability spanning one order of magnitude, and all SFTTAs with various scales show an excellent twisting capability. A baseline SFTTA prototype

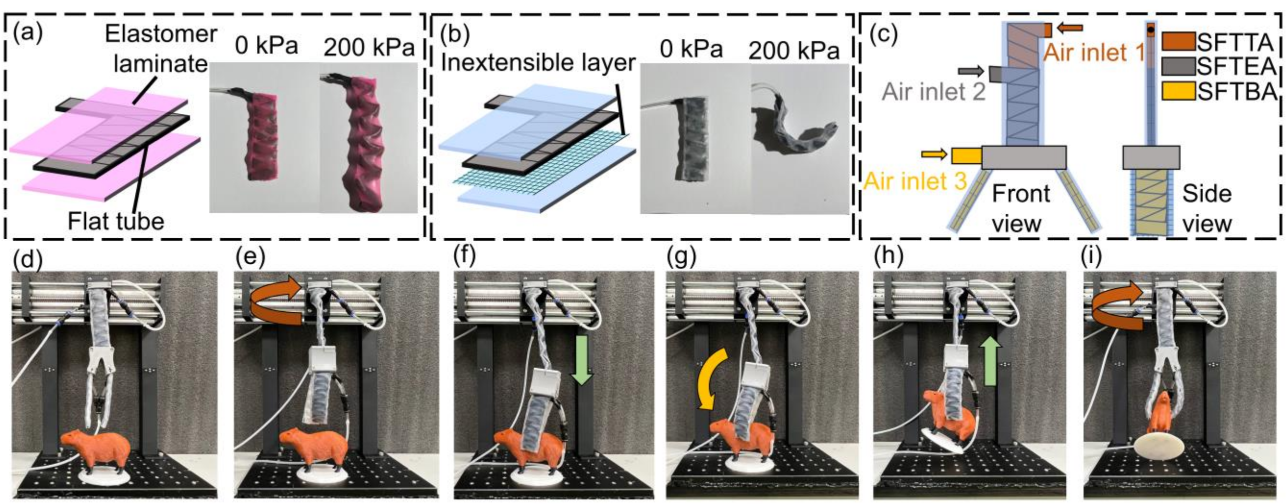

Figure 7. Soft robotic gripper based on the soft flat tube actuators. (a) Structure and prototype of the SFTEA. (b) Structure and prototype of the SFTBA. (c) Structure of the soft gripper. (d) Prototype of the soft gripper. (e) Twisting actuation provided by SFTTA. (f) Extending actuation provided by SFTEA. (g) Grasping motion actuation provided by SFTBA. (h) Lifting the object by deflating the SFTEA. (i) Rotating the object by deflating the SFTTA.

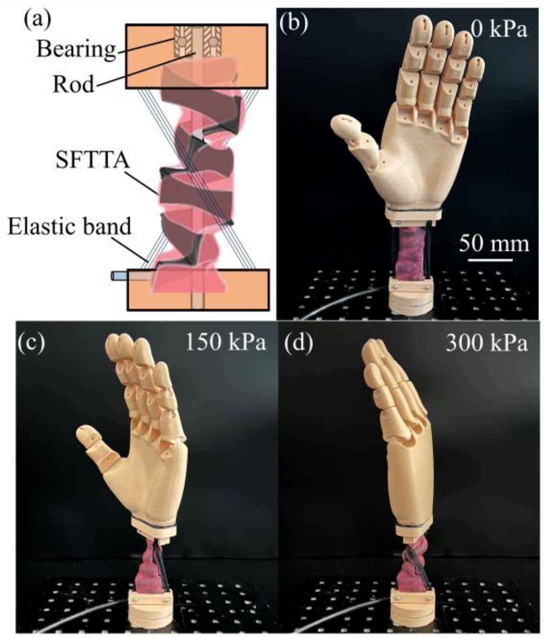

Figure 8. Robotic wrist module based on the SFTTA. (a) Robotic wrist module. (b) Robotic wrist module assembled on a hand model at the initial state. (c, d) Robotic wrist module actuated under 150 kPa and 300 kPa.

can twist up to 540 degrees. The smallest SFTTA prototype only has a length of 24 mm, and it can twist 9.6 °/mm, which is far larger than previous soft twisting actuators. The torque output capability of the SFTTA is better than that of origami actuators [19] but less than that of fiber-reinforced soft actuators and fabric-based actuators, [11,12] and the torque output is proportional to the cross-section area of the actuator. Changing the pattern of the folded corner of the flat tube and the material of the laminate can transfer the SFTTA to extending and bending actuators, which are named soft flat tube extending actuator (SFTEA) and soft flat tube bending actuator (SFTBA), respectively.

There are some limitations and potential development opportunities. Firstly, different materials of the flat tube can be selected and tested. Although the ventilation problem of the SFTTA is solved by a single PE fishing line, the response time and recovery time are still too slow, which could be optimized using a D-shape thermoplastic polyurethane (TPU) or silicone rubber tube. Secondly, this study focused on the twisting actuator, and we also introduced novel extending and bending actuators without further study and discussion. The bonding between the elastomer and flat tube folding patterns is a promising research direction as more motions can be developed using this combination. Besides, modeling of the SFTTA is required to achieve precise rotation angle control in the future study.

References

[1] D. Rus and M. T. Tolley, "Design, fabrication and control of Soft Robots," *Nature*, vol. 521, no. 7553, pp. 467–475, May 2015.

[2] J. Shintake, V. Cacucciolo, D. Floreano, and H. Shea, "Soft robotic grippers," *Advanced Materials*, vol. 30, no. 29, p. 1707035, May 2018.

[3] W. Zhu et al., "A Soft-Rigid Hybrid Gripper With Lateral Compliance and Dexterous In-Hand Manipulation," *IEEE/ASME Transaction on Mechatronics*, vol. 28, no. 1, pp. 104-115, Feb. 2023.

[4] P. Polygerinos, Z. Wang, K. C. Galloway, R. J. Wood, and C. J. Walsh, "Soft robotic glove for combined assistance and at-home rehabilitation," *Robotics and Autonomous Systems*, vol. 73, pp. 135–143, Nov. 2015.

[5] H. Liu et al., "Finger flexion and extension driven by a single motor in Robotic Glove Design," *Advanced Intelligent Systems*, vol. 5, no. 5, Feb. 2023.

[6] M. Wehner et al., "An integrated design and fabrication strategy for entirely soft, autonomous robots," *Nature*, vol. 536, no. 7617, pp. 451–455, Aug. 2016.

[7] Y. Li, F. Fish, Y. Chen, T. Ren, and J. Zhou, "Bio-inspired robotic dog paddling: Kinematic and Hydro-dynamic analysis," *Bioinspiration and Biomimetics*, vol. 14, no. 6, p. 066008, Sep. 2019.

[8] Q. Shao et al., "Untethered Robotic Millipede Driven by Low-Pressure Microfluidic Actuators for Multi-Terrain Exploration," *IEEE Robotics and Automation Letters*, vol. 7, no. 4, pp. 12142-12149, Oct. 2022.

[9] Y. Lin, Y.-X. Xu, and J.-Y. Juang, "Single-actuator soft robot for in-pipe crawling," *Soft Robotics*, vol. 10, no. 1, pp. 174–186, Feb. 2023.

[10] F. Connolly, C. J. Walsh, and K. Bertoldi, "Automatic design of fiber-reinforced soft actuators for trajectory matching," *Proceedings of the National Academy of Sciences*, vol. 114, no. 1, pp. 51–56, Dec. 2016.

[11] P. H. Nguyen and W. Zhang, "Design and computational modeling of Fabric Soft Pneumatic actuators for wearable assistive devices," *Scientific Reports*, vol. 10, no. 1, Jul. 2020.

[12] F. Connolly, P. Polygerinos, C. J. Walsh, and K. Bertoldi, "Mechanical programming of soft actuators by varying fiber angle," *Soft Robotics*, vol. 2, no. 1, pp. 26–32, Mar. 2015.

[13] R. V. Martinez, C. R. Fish, X. Chen, and G. M. Whitesides, "Elastomeric Origami: Programmable paper-elastomer composites as pneumatic actuators," *Advanced Functional Materials*, vol. 22, no. 7, pp. 1376–1384, Feb. 2012.

[14] Z. Jiao, C. Ji, J. Zou, H. Yang, and M. Pan, "Vacuum-powered soft pneumatic twisting actuators to empower new capabilities for Soft Robots," *Advanced Materials Technologies*, vol. 4, no. 1, p. 1800429, Oct. 2018.

[15] S. Kurumaya et al., "A modular soft robotic wrist for underwater manipulation," *Soft Robotics*, vol. 5, no. 4, pp. 399–409, Aug. 2018.

[16] S. Sanan, P. S. Lynn, and S. T. Griffith, "Pneumatic torsional actuators for inflatable robots," Journal of Mechanisms and Robotics, vol. 6, no. 3, Apr. 2014.

[17] W. Xiao, D. Hu, W. Chen, G. Yang, and X. Han, "A new type of soft pneumatic torsional actuator with Helical Chambers for Flexible Machines," *Journal of Mechanisms and Robotics*, vol. 13, no. 1, Aug. 2020.

[18] F. Chen, Y. Miao, G. Gu and X. Zhu, "Soft Twisting Pneumatic Actuators Enabled by Freeform Surface Design," *IEEE Robotics and Automation Letters*, vol. 6, no. 3, pp. 5253-5260, July 2021.

[19] W. Xiao et al., "Cooperative collapse of helical structure enables the actuation of twisting pneumatic artificial muscle," *International Journal of Mechanical Sciences*, vol. 201, p. 106483, Jul. 2021.

[20] B. Gorissen et al., "Flexible pneumatic twisting actuators and their application to tilting micromirrors," *Sensors and Actuators A: Physical*, vol. 216, pp. 426–431, Sep. 2014.

[21] J. T. Waters et al., "Twist again: Dynamically and reversibly controllable chirality in liquid crystalline elastomer microposts," *Science Advances*, vol. 6, no. 13, Mar. 2020.

[22] J.E. Shim et al., "A smart soft actuator using a single shape memory alloy for twisting actuation," *Smart Materials and Structures*, vol. 24, no. 12, p. 125033, Nov. 2015.

[23] N. Kellaris, V. Gopaluni Venkata, G. M. Smith, S. K. Mitchell, and C. Keplinger, "Peano-Hasel actuators: Muscle-mimetic, electrohydraulic transducers that linearly contract on activation," *Science Robotics*, vol. 3, no. 14, Jan. 2018.

[24] H. Liu, C. Wu, S. Lin, and Y. Chen, "Finger joint aligned flat tube folding structure for robotic glove design," *Smart Materials and Structures*, vol. 33, no. 1, p. 015001, Dec. 2023.

[25] J. Yan, X. Zhang, B. Xu, and J. Zhao, "A new spiral-type inflatable pure torsional soft actuator," Soft Robotics, vol. 5, no. 5, pp. 527–540, Oct. 2018.